metals

MDPI

Article

Corrosion Behavior of Passivated CUSTOM450 and AM350 Stainless Steels for Aeronautical Applications

Oliver Samaniego-Gámez [1], Facundo Almeraya-Calderón [1,*], José Chacón-Nava [2], Erick Maldonado-Bandala [3], Demetrio Nieves-Mendoza [3], Juan Pablo Flores-De los Rios [4], Jesús Manuel Jáquez-Muñoz [1], Anabel D. Delgado [2] and Citlalli Gaona-Tiburcio [1,*]

[1] Universidad Autonoma de Nuevo Leon, FIME-Centro de Investigación e Innovación en Ingeniería Aeronáutica (CIIIA), Av. Universidad s/n, Ciudad Universitaria, San Nicolás de los Garza 66455, Mexico; pedro.samaniegogm@uanl.edu.mx (O.S.-G.); jesus.jaquezmn@uanl.edu.mx (J.M.J.-M.)

[2] Department of Metallurgy and Structural Integrity, Centro de Investigación en Materiales Avanzados (CIMAV), Miguel de Cervantes 120, Complejo Industrial Chihuahua, Chihuahua 31136, Mexico; jose.chacon@cimav.edu.mx (J.C.-N.); anabel.delacruz@cimav.edu.mx (A.D.D.)

[3] Facultad de Ingeniería Civil, Universidad Veracruzana, Xalapa 91000, Mexico; erimaldonado@uv.mx (E.M.-B.); dnieves@uv.mx (D.N.-M.)

[4] Department Metal-Mechanical, Tecnológico Nacional de Mexico-Instituto Tecnológico de Chihuahua, Av. Tecnologico 2909, Chihuahua 31130, Mexico; juan.fd@chihuahua.tecnm.mx

* Correspondence: facundo.almerayacld@uanl.edu.mx (F.A.-C.); citlalli.gaonatbr@uanl.edu.mx (C.G.-T.)

Abstract: Custom 450 stainless steel and AM 350 stainless steel are both precipitation hardening stainless steels, which are widely used in a variety of aerospace applications. The former steel exhibits very good corrosion resistance with moderate strength, whereas the latter is used for applications requiring high strength along with corrosion resistance. In this study, the corrosion behavior of CUSTOM 450 and AM 350 stainless steels passivated in (a) citric acid and (b) nitric acid solutions for 50 and 75 min at 49 and 70 °C, and subsequently exposed in 5 wt. % NaCl and 1 wt. % H_2SO_4 solutions are investigated. Two electrochemical techniques were used: electrochemical noise (EN) and electrochemical impedance spectroscopy (EIS) according to ASTM G199-09 and ASTM G106-13, respectively. The results indicated that passivation in nitric acid made the surface prone to localized corrosion. Statistical and PSD values showed a tendency toward pitting corrosion. On the whole, passivated CUSTOM 450 stainless steel showed the best corrosion behavior in both, NaCl and H_2SO_4 test solutions.

Keywords: PH stainless steel; passivation baths; electrochemical noise; electrochemical impedance spectroscopy

1. Introduction

Nowadays, stricter environmental regulations suggest the need to seek environmentally-friendly corrosion protection processes in the aeronautical sector. Passivation is a chemical treatment typically for stainless steel that enhances the ability of the treated surfaces to resist corrosion [1–6].

Stainless steels (SS are widely used in aircraft components due to their very good mechanical properties, weldability, thermal expansion, impact resistance, and corrosion resistance, among others). According to their chemical composition and metallurgical phases, stainless steels are classified into five families, i.e. austenitic, ferritic, martensitic, duplex (consisting of a mixture of ferrite and austenite), and PH (precipitation hardened) [5,7]. Typically, austenitic, martensitic, and PH stainless steels are used in the aeronautical industry. Their corrosion, mechanical and high-temperature properties allow them to perform well in aggressive environments and makes them suitable for various aircraft parts, such as landing gear supports, actuators, and fasteners [6,8].

The precipitation-hardening (PH) stainless steels are a family of corrosion-resistant alloys some of which can be heat-treated to provide tensile strengths well above 850 MPa and yield strengths well above 520 MPa. These steels have chromium (11 to 18%), Nickel (3 to 4%) as main alloying elements, and small amounts of other metals, such as molybdenum (this element increases the corrosion resistance, in particular, the pitting corrosion resistance), aluminum, titanium, niobium, and tungsten. Chromium is essential for forming the protective passivation layer [9,10]. The addition of other alloying elements helps to improve the quality of the passivation layer. Nickel is the second essential element in stainless steel, which helps to stabilize the austenitic phase, and also improves mechanical properties [11,12]. PH stainless steels can be divided into martensitic, austenitic, and semi-austenitic. These steels are widely used in structural components in aircraft due to their excellent resistance to corrosion and high toughness due to the formation of precipitates (hard intermetallic compounds) after an age-hardening treatment [13–18]. The aeronautical and aerospace industry has been used PH stainless steels such as 17-4PH, 15-7Mo, 15-5PH, and more recently AM350 and AM355 (Allegheny Ludlum Inc., Pittsburgh, PA, USA), CUSTOM450, and CUSTOM455 (Carpenter Tech. Corp., Odessa, TX, USA) [19,20].

All stainless steels contain chromium, which reacts with oxygen and moisture in the environment to form a protective, adherent, and coherent oxide film on the material surface. This oxide film (passive layer) is very thin (2–3 nanometers thick). According to ASTM A967 [21], passivation is the chemical treatment of stainless steel with an oxidant agent, to remove free iron or other materials. The passivation baths commonly use citric and nitric acid as oxidizing agents. However, the latter generates toxic vapors that are harmful to health [22–24]. On the other hand, citric acid is considered a biodegradable alternative that does not generate hazardous waste. Although some benefits of the passivation process with citric acid can be expected, technical information in the literature is scarce [25–27]. Back in 2003, the Boeing Company [6] studied citric acid as an alternative for stainless steel passivation. A study conducted by the National Aeronautics and Space Administration (NASA) in 2003 made it possible to evaluate the use of nitric acid in the passivation process of welded materials using the salt chamber technique [10]. Subsequently, NASA evaluated the use of citric acid in samples exposed to atmospheric corrosion and evaluated the passive layer's adhesion [21].

Important parameters such as passivation range, transpassive regions, pitting nucleation potentials, corrosion rates, and corrosion mechanisms in stainless steels have been studied by electrochemical techniques such as galvanostatic, potentiostatic, and potentiodynamic polarization, electrochemical impedance spectroscopy (EIS) and electrochemical noise (EN) [26].

Bragaglia et al. [27] studied by potentiodynamic polarization the behavior of passivated and unpassivated AISI 304 austenitic stainless steel in citric and nitric acid baths, and they reported that the passivation treatment significantly increased the pitting potential, particularly in nitric acid. After 24 h of exposure, the corrosion behavior of the passivated samples in the acid baths was almost identical. Suresh and Mudali [28] studied the corrosion of AISI 304 stainless steel in 0.05 M ferric chloride ($FeCl_3$) solution by electrochemical noise to investigate the corrosion mechanism. They found a relationship with the roll-off slopes derived from power spectral density analysis and statistical analysis such as standard deviation (SD), localization index (LI), and kurtosis with pitting as the corrosion mechanism. Lara et al. [29] studied the electrochemical behavior of 15-5PH and 17-4PH passivated stainless steels by electrochemical noise (EN) and potentiodynamic polarization curves (PPC). The results indicated that these steels formed a similar passive layer in both, nitric and citric acid solutions.

CUSTOM 465 is a martensitic and age-hardenable stainless steel that has been a relatively new addition to the family of PHSS. AM-350 alloy is a semi-austenitic type precipitation hardening stainless steel, with similar characteristics to those of the AISI 300 series stainless steels. Recent investigations on CUSTOM450 and AM350 steels have focused

on fatigue behavior, hydrogen diffusion, microstructural characterization, machinability, and there are only a few works on pitting corrosion kinetics [30–37].

The aim of this work is to evaluate the corrosion behavior of the CUSTOM450 and AM350 stainless steels passivated in citric and nitric acid solutions for 50 and 75 min at 49 and 70 °C, and subsequently exposed in 5 wt. % NaCl and 1 wt. % H_2SO_4 solutions. Two electrochemical techniques were used: electrochemical noise (EN) and electrochemical impedance spectroscopy (EIS). Martensitic stainless steel they are precipitation-hardenable alloy used in aeronautics and exposed to different atmospheres such as marine and industrial (acid rain).

2. Materials and Methods

2.1. Materials

The materials used in this work were CUSTOM450 (UNS S45000) and AM350 (UNS35000) stainless steel, tested in the as-received condition. The nominal chemical composition of these stainless steels [38,39] is shown in Table 1.

Table 1. Chemical composition of the CUSTOM450 and AM350 SS (wt. %).

Elements	Stainless Steel Alloys	
	CUSTOM450	AM350
Cr	14.0–16.0	16.0–17.0
Ni	5.0–7.0	4.0–5.0
Mo	0.50–1.0	2.50–3.25
Mn	1.00	0.50–1.25
Cu	1.25–1.75	–
Ti	0.90–1.40	–
Nb	0.5–0.75	–
N	≤0.1	0.07–0.13
Si	1.00	≤0.50
S	0.030	0.030
C	≤0.05	0.07–0.11
Fe	Balance	Balance

Stainless steels samples were prepared according to ASTM E3-11 (2017) [40]. The various alloys were ground using 400, 600, and 800 grade SiC sandpaper followed by ultrasonic cleaning in ethanol (C_2H_5OH) and deionized water for 10 min for each sample.

2.2. Passivation Process

The passivation process was carried out under ASTM A967-17 [21]. Gaydos et al. [22] reported that extended passivation treatments gave better protection against corrosion for a series of stainless steels. The passivation treatment consisted of the following stages:

1. Pretreatment: degreased and pickling in a 50 wt.% HCl solution (analytical grade reagents (J.T. Baker, Nuevo León, México) for 5 s at 25 °C and rinsed in distilled water [41]).
2. The different combinations of citric and nitric acid baths available for testing were too many, so a 3-factor, 2-tier design of experiment 5 (DoE) was conducted to determine the optimal concentration of citric and nitric acid. The temperature of the solution and the passivation time.
3. Passivation treatment: two passivation baths of nitric acid (20%*v*) and citric acid (55%*v*) solutions were used. A constant temperature of 49 and 70 °C was maintained through the passivation process. Specimens were immersed in the solutions for 50 and 75 min.
4. Final treatment: Rinsed in distilled water.

Table 2 shows the passivation exposure conditions for each type of HP stainless steel.

Table 2. Nomenclature and passivation process parameters.

Alloys	Passivation Baths	Time (min)	Temperature (°C)	Nomenclature *
AM350	$C_6H_8O_7$	50	49	AM350-CA-75min-49 °C
	HNO_3	50	70	AM350-NA-50min-70 °C
	HNO_3	50	70	AM350-NA-50min-70 °C
	$C_6H_8O_7$	75	49	AM350-CA-75min-49 °C
CUSTOM450	HNO_3	75	70	CUSTOM450-NA-75min-70 °C
	HNO_3	50	49	CUSTOM450-NA-50min-49 °C
	$C_6H_8O_7$	50	49	CUSTOM450-CA-50min-49 °C
	$C_6H_8O_7$	75	49	CUSTOM450-CA-75min-49 °C

* Nitric acid (NA) and citric acid (CA).

2.3. Electrochemical Tests

Electrochemical measurements were conducted at room temperature using an electrochemical interface mod. 1287A and Impedance Analyzer mod. Then 1260 Solartron (Bognor Regis, UK) two 5 wt. % NaCl and 1 wt. % H_2SO_4 solutions were used with the latter reagent used to simulate acid rain conditions [5]. A conventional three-electrode cell configuration was used for the electrochemical corrosion studies, which consisted of a working electrode, WE (passivated CUSTOM450 and AM350 steels), a reference electrode, RE (calomel electrode (SCE)), and an auxiliary electrode, CE (platinum mesh) [6,42,43]. Before the test, the working electrode (passivated stainless steel sample) was held for about 1 h at open circuit potential (OCP). Corrosion tests were realized in triplicate.

EIS test parameters were used in the range of 100 kHz to 1 mHz, with an amplitude of 10 mV sinewave [44–48]. The impedance data were collected and modeled using ZPlot and ZView software (Zview 2.0 software), respectively (Scribner Associates, Southern Pines, NC, USA).

Electrochemical noise (EN) measurements of current and potential values at one-second intervals on the passivated stainless steel tested were taken. The time records consisted of 1024 data. The electrochemical cell for EN measurements consisted of an array of three electrodes: PHSS samples (working electrode WE1), a platinum electrode (WE2), and a saturated calomel electrode as reference electrode (RE). The EN data were detrended using a degree 9 polynomial and applying the fast Fourier transform (FFT) with a Hann window [49–54]. Data processing was performed with a program that can be used in MATLAB 2018a software (Math Works, Natick, MA, USA) [55–57].

3. Results

3.1. Electrochemical Measurements

3.1.1. Electrochemical Noise Analysis

The electrochemical noise (EN) technique is non-perturbative and describes the spontaneous low-level potential and current fluctuations during an electrochemical process. During the corrosion process, predominantly electrochemical anodic and cathodic reactions can cause small transients in the electrical charges of the material under study.

Figure 1 shows the time series obtained for the passivated steels after exposure to the NaCl electrolyte. Figure 1a shows the electrochemical potential noise (EPN), where all samples show a decrease in amplitude over time. This behavior can be related to a decrease in ionic exchange due to thermodynamic stabilization. Sample anodized in nitric acid AM350-NA-50 min-70 °C showed a higher potential amplitude (3×10^{-2} V).

Figure 1b shows the electrochemical current noise (ECN), where the behavior of CUSTOM450-CA-50 min-49 °C, which in these conditions shows the higher amplitude fluctuations This behavior can be related to the higher corrosion kinetic of the passive layer in this condition, and the maximum value is 2.5×10^{-5} A/cm^2. On the other hand, AM350-CA-50min-49 °C and AM350-NA-50min-70 °C presented the lowest amplitude value of about $\times 10^{-7}$ A/cm^2. This result can be related to its corrosion resistance in NaCl.

The passivated AM350 steel is more corrosion resistant than passivated CUSTOM 450 steel when these steels are exposed to NaCl.
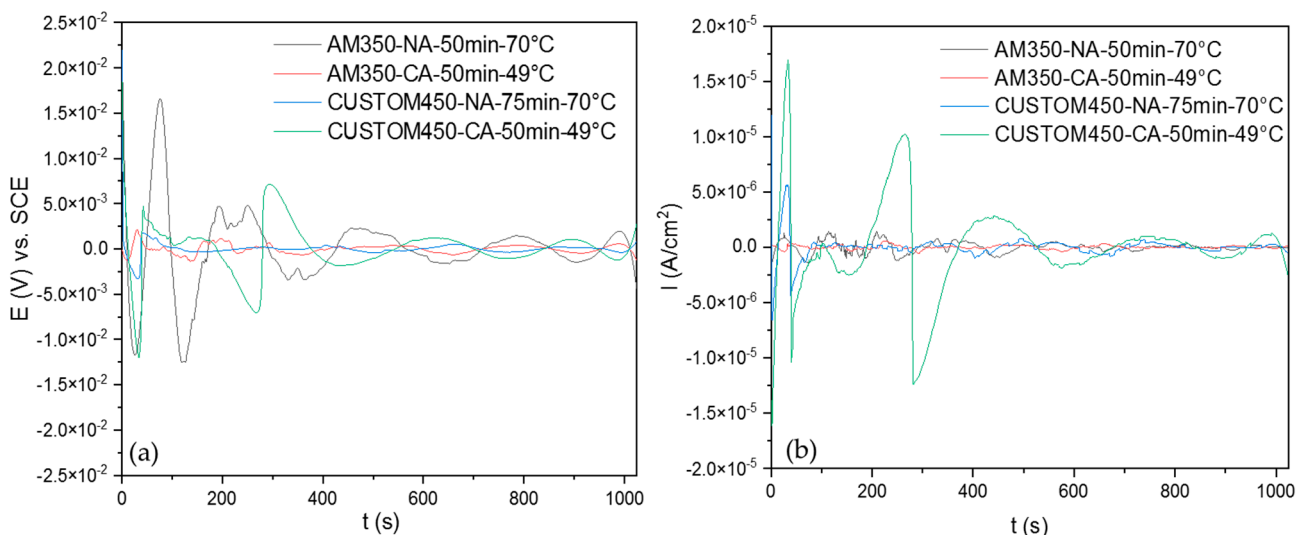

Figure 1. Electrochemical noise–time series: (**a**) EPN and (**b**) ECN, for CUSTOM450 and AM350 passivated stainless steels immersed in 5 wt. % NaCl solution.

Figure 2a shows the EPN time series when passivated steels are exposed to H_2SO_4. The ionic exchange is of low order ($\times 10^{-5}$ V). The low fluctuation amplitude is related to a generation of the passive layers created by the H_2SO_4 electrolyte. As can be seen, all samples presented the same behavior. Figure 2b shows the EPN time series where the sample anodized in citric acid AM350-CA-75min-49 °C presents the higher current transients of 1.5×10^{-6} A/cm^2. Meanwhile, CUSTOM450-NA-75min-70 °C presented transients of 8×10^{-7} A/cm^2, related to localized processes, but they occur due to the passive layer's breakdown and regeneration. Furthermore, a transitory reaction is induced by a non-uniform passive layer, and OH— reactions occur easier. The results show that passivated AM350-CA-75min-49 °C and passivated CUSTOM450-CA-50min-49 °C are more susceptible to pitting corrosion.
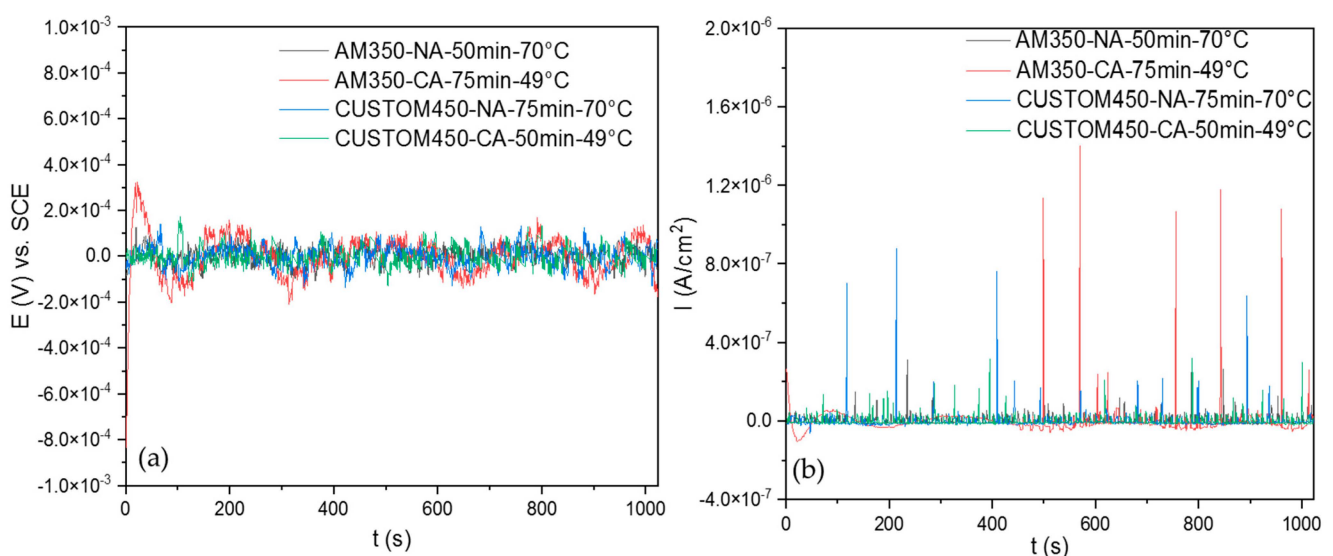

Figure 2. Electrochemical noise–time series: (**a**) EPN and (**b**) ECN, for CUSTOM 450 and AM 350 passivated stainless steels immersed in 1 wt. % H_2SO_4 solution.

Statistical Analysis

EN can be studied by various methods such as time domain, where analysis is made by visual analysis, skewness, localization index (LI), and noise resistance (R_n). Another method to study EN signals is by power spectral density (PSD); this method evaluates frequency signals. Nevertheless, since the EN shows different signals (see Equation (1)), it is necessary to separate components that do not provide any information about the corrosion process. The DC (m_t) component can be separated by different methods, such as the polynomial filter or wavelets. The random (S_t) and stationary (Y_t) components are considered because the corrosion process occurs in those signals [58–62].

$$x(t) = m_t + s_t + Y_t \tag{1}$$

To determine noise resistance (R_n) it is necessary to obtain the standard deviation from time series values; these statistical values give corrosion kinetics and mechanistic information. Cottis and Turgoose [53] found a relationship between an increase in variance and standard deviation with increased corrosion rate. For standard deviation, (σ) evaluation applying Equation (1) is required, for which Rn can be obtained (Equation (2)) using the relationship between the standard deviations from EN potential (σ_E), and current signals (σ_I):

$$R_n = \frac{\sigma_E}{\sigma_I} \tag{2}$$

The statistical analysis (Table 3) showed that mixed corrosion is predominant in both electrolytes. Only AM350-NA-50min-70 °C and CUSTOM450-NA-50min-49 °C systems showed localized corrosion when exposed to sulfuric acid, which can be related to a non-uniform layer. However, when steels under passivation conditions are exposed to NaCl, only CUSTOM450-NA-75min-70 °C showed mixed corrosion, corrosion, and the other samples presented uniform corrosion. Skewness shows that localized processes are predominant in corrosion systems due to passive layer generation. Furthermore, the samples passivated in citric acid presented a lower corrosion resistance. However, samples passivated in nitric acid presented a non-uniform passive film due to localized corrosion.

Table 3. EN statistical parameters from passivated CUSTOM 450 and AM 350 stainless steels.

Electrolyte	Sample	R_n (ohm)	LI	Type of Corrosion	Skewness	Type of Corrosion
NaCl	AM350-NA-50min-70 °C	8737	0.009	Uniform	−0.23	Uniform
	AM350-CA-50min-49 °C	3047	0.003	Uniform	0.14	Uniform
	CUSTOM450-NA-75min-70 °C	689	0.028	Mixed	0.21	Uniform
	CUSTOM 450-CA-50min-49 °C	884	0.005	Uniform	2	Localized
H$_2$SO$_4$	AM350-NA-50min-70 °C	1571	0.2	Localized	1.7	Localized
	AM350-CA-75min-49 °C	1055	0.04	Mixed	2.4	Localized
	CUSTOM 450-CA-75min-49 °C	849	0.07	Mixed	1.78	Localized
	CUSTOM 450-NA-50min-49 °C	1478	0.16	Localized	2.7	Localized

Power Spectral Density Analysis and Noise Impedance (Z_n)

The separation of the DC signal is necessary because DC creates false frequencies and interferes in visual, statistical, and PSD analysis. The polynomial method is governed by Equation (3), where x_n is the EN signal with all the components, a polynomial of "n" grade (p_o) at n-th term (a_i) in „n" time to obtain a signal without trend (y_n) [53,54]. In this work, a 9th-degree polynomial was applied.

$$y_n = x_n - \sum_{i=0}^{p_o} a_i n^i \tag{3}$$

For power spectral density (PSD) analysis, it is necessary to apply a polynomial filter to the original signal, followed by the application of a fast Fourier transform (FFT) to transform from time to frequency domain. Equations (4) and (5) are employed to obtain spectral densities [47–60].

$$R_{xx}(m) = \frac{1}{N} \sum_{n=0}^{N-m-1} x(n) \cdot x(n+m), \text{ when values are from } 0 < m < N \qquad (4)$$

$$\Psi_x(k) = \frac{\gamma \cdot t_m}{N} \cdot \sum_{n=1}^{N} (x_n - \bar{x}_n) \cdot e^{\frac{-2\pi k n^2}{N}} \qquad (5)$$

The interpretation of PSD is based on the slope and frequency zero limits (Ψ^0). The slope is related to the type of corrosion present in the system [35,36]. The slope is mathematically defined by β_x and is represented by Equation (6):

$$log\Psi_x = -\beta_x \log f \qquad (6)$$

To obtain information about the material dissolution, it is required to analyze the frequency zero limits (Ψ^0) in current PSD [24]. The following table helps to determine the corrosion process in a given system [60–64]. Results of Table 4 show the parameters obtained from the first test because in general experiments did not show any significant variations.

Table 4. β intervals to indicate the type of corrosion [47].

Corrosion Type	dB(V)·Decade^{-1}		dB(A)·Decade^{-1}	
	Minimum	**Maximum**	**Minimum**	**Maximum**
Uniform	0	−7	0	−7
Pitting	−20	−25	−7	−14
Passive	−15	−25	−1	1

The spectral noise resistance is the noise impedance (Zn), which is expressed by the following equations [6,47,62,65]

$$Z_n = \sqrt{\frac{\psi_V(f)}{\psi_I(f)}} \qquad (7)$$

Noise impedance is calculated as the square root of the ratio of the PSD of EPN divided by the PSD of ECN. The electrochemical noise impedance zero (Z_n0) is related to corrosion resistance [59,66].

Figure 3a shows the PSD of the ECN. Sample CUSTOM450-CA-50min-49 °C has the highest corrosion dissolution with −99.05 dBi, and a lower noise impedance of 856 $\Omega \cdot cm^2$ (see Table 5); these results may be related to high corrosion kinetics. On the other hand, Figure 3b sample AM350-NA-50min-70 °C showed a higher noise impedance value (75,382 $\Omega \cdot cm^2$) and lower material dissolution with −129.55 dBi (see Table 5). All the slope values are related to pitting corrosion when exposed to NaCl.

Figure 4 a shows the current PSD, and sample AM350-CA-75min-49 °C showed the higher corrosion kinetic even in Figure 4a with −128.66 dBi. The passivated steel that showed the lower noise impedance value was CUSTOM450-CA-50min-49 °C (1972 $\Omega \cdot cm^2$). (Figure 4b) Compared to samples passivated in nitric acid and exposed to sulfuric acid, those passivated in citric acid presented lower corrosion resistance. Samples passivated with nitric acid presented a better performance in both NaCl and H_2SO_4 solutions.

Table 5 shows that all samples exposed to NaCl presented pitting corrosion. The results obtained by statistical analysis showed a uniform system. This behavior may be related to a uniform distribution of pitting. When samples were exposed to H_2SO_4, uniform corrosion occurred on the sample surface. This process could be attributed to the uniform breakdown and regeneration of the passive layer.
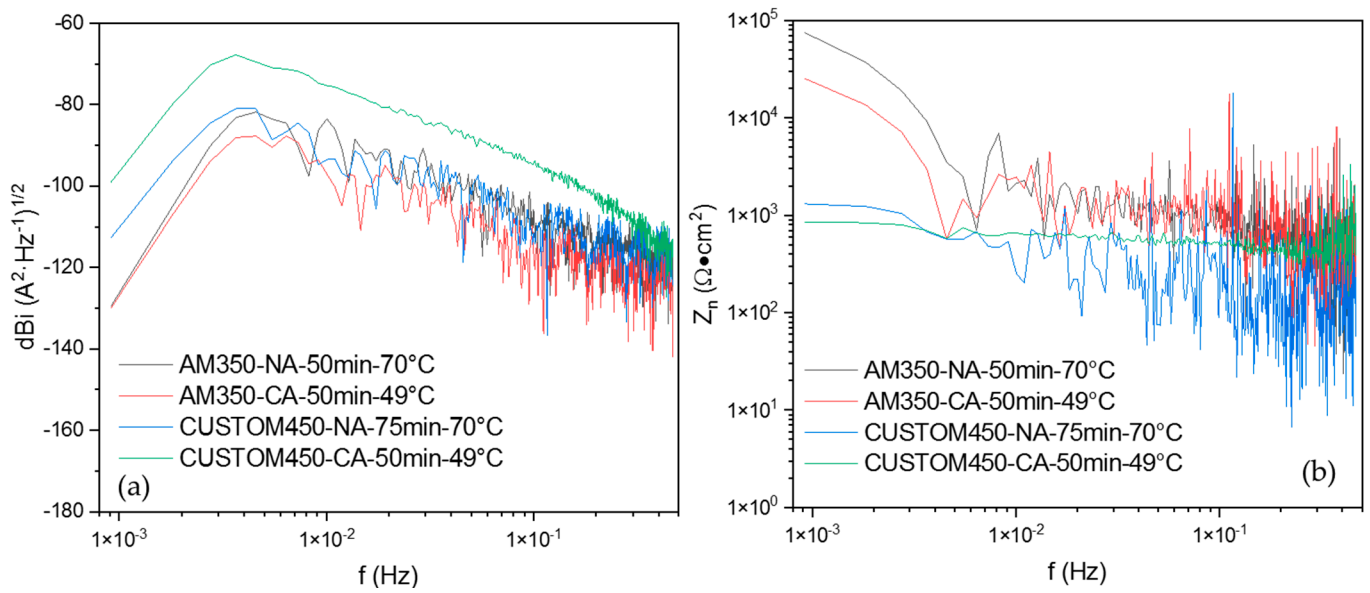
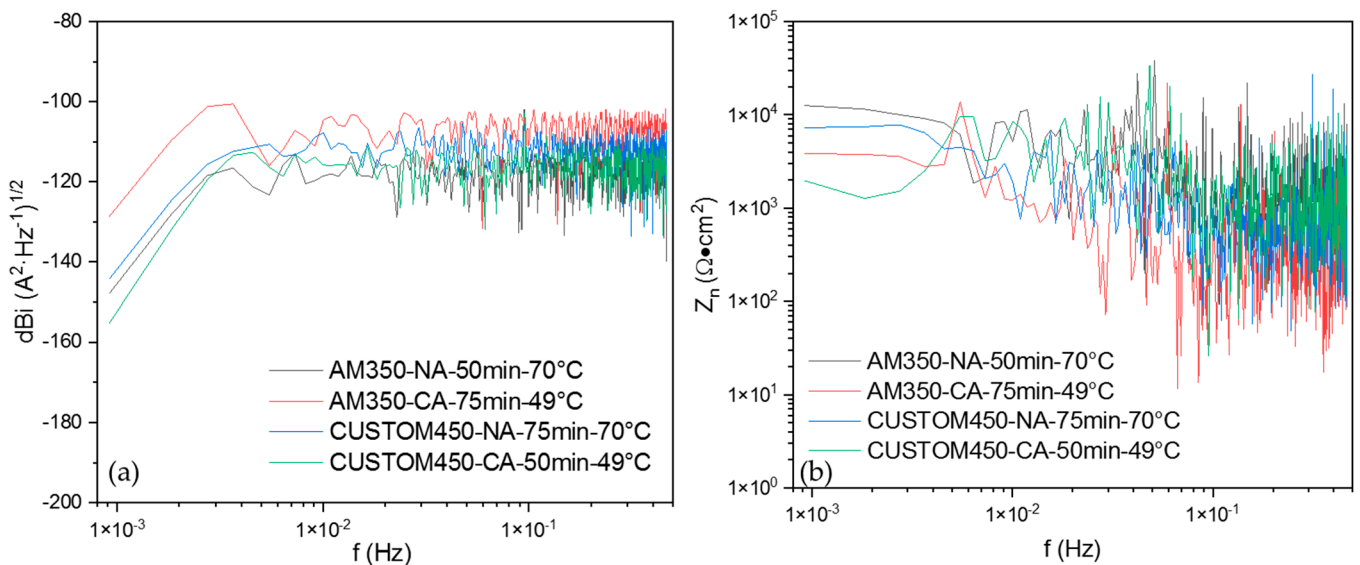**Figure 3.** (**a**) Power spectral density (PSD) and (**b**) Noise impedance (Z_n) for CUSTOM450 and AM 350 passivated stainless steels immersed in 5 wt. % NaCl solution.

Table 5. Parameters obtained by PSD.

Solutions	Sample	B (dB (A))	Z_n0 ($\Omega \cdot cm^2$)	Type of Corrosion	Ψ^0 (dBi)
NaCl	AM350-NA-50min-70 °C	−14	75,386	Localized	−129.553369
	AM350-CA-50min-49 °C	−12	25,491	Localized	−129.977241
	CUSTOM450-NA-75min-70 °C	−21	856	Localized	−99.0505805
	CUSTOM 450-CA-50min-49 °C	−13	1309	Localized	−112.691823
H_2SO_4	AM350-NA-50min-70°C	2	12,574	Uniform	−147.88788
	AM350-CA-75min-49°C	1	3832	Uniform	−128.661037
	CUSTOM 450-CA-75min-49°C	1	7294	Uniform	−144.250449
	CUSTOM 450-NA-50min-49°C	2	1972	Uniform	−155.287684

Figure 4. (**a**) Power spectral density (PSD) and (**b**) noise impedance (Z_n) for CUSTOM 450 and AM 350 passivated stainless steels immersed in 1 wt. % H_2SO_4 solution.

3.1.2. Electrochemical Impedance Spectroscopy Analysis

Electrochemical impedance spectroscopy (EIS) has been widely used to study the electrochemical mechanisms at electrodes. The characteristics of the EIS spectra of the samples investigated in the present study are presented in Figures 5 and 6 which show Nyquist and Bode plots for AM350 y CUSTOM 450 passivated stainless steels and immersed in 5 wt. % NaCl and 1 wt. % H_2SO_4 solution. The EIS analysis was employed to analyze the corrosion susceptibility and protection properties of passivated HPSS and electrochemical noise. The electrochemical behavior of passivated HPSS may be due to an oxide layer with a constant phase element and a combination of resistive elements in the equivalent circuit. The aforementioned behavior can be seen in the Bode plots through the phase angle distribution. This is the case with untreated stainless steel, as they naturally form a barrier layer when exposed to oxygen from the environment. In the NaCl solution, the passivated alloy in citric acid may have a higher charge transfer resistance (AM350-CA-50min-49 °C and CUSTOM 450-NA-50min-49 °C). The CUSTOM 450-CA-75min-49 °C sample immersed in H_2SO_4 had the highest charge transfer resistance i.e., 4.252×10^6 $\Omega \cdot cm^2$ passivated in a citric acid bath, and the lower value corresponding to sample AM350 (NA 20 wt. %; 50 min; 70 °C) with a value of 3.915×10^4 $\Omega \cdot cm^2$, respectively. All impedance spectra have the same EIS measurement frequency range characteristics. Figures 5b,c and 6b,c show the Bode plots for all impedance data, one peak can be observed in the phase angle (θ) vs. frequency plot, indicating that HPSS passivated presents one-time constants.
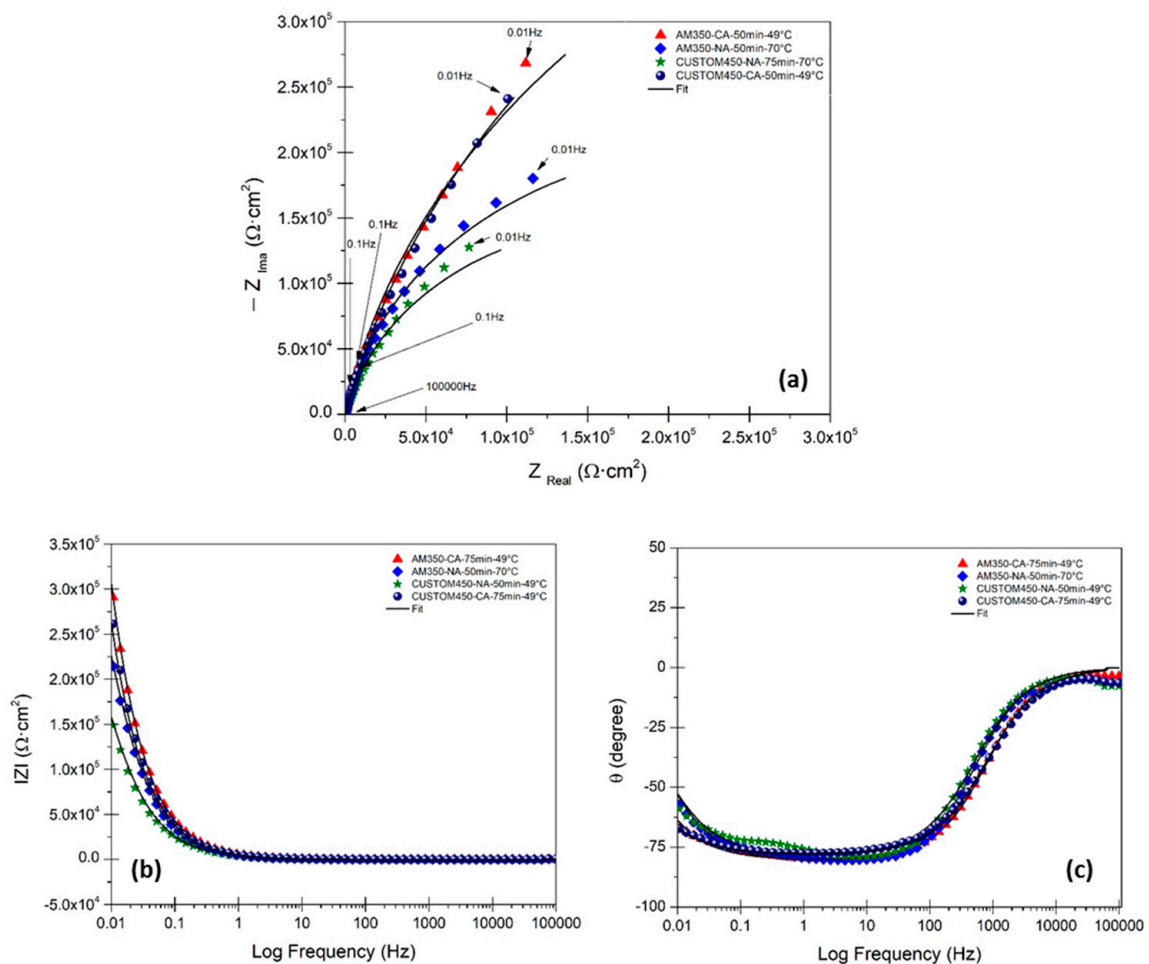

Figure 5. Nyquist (**a**) and Bode (**b**,**c**) plots of CUSTOM 450 and AM 350 passivated stainless steels immersed to 5 wt. % NaCl solution.
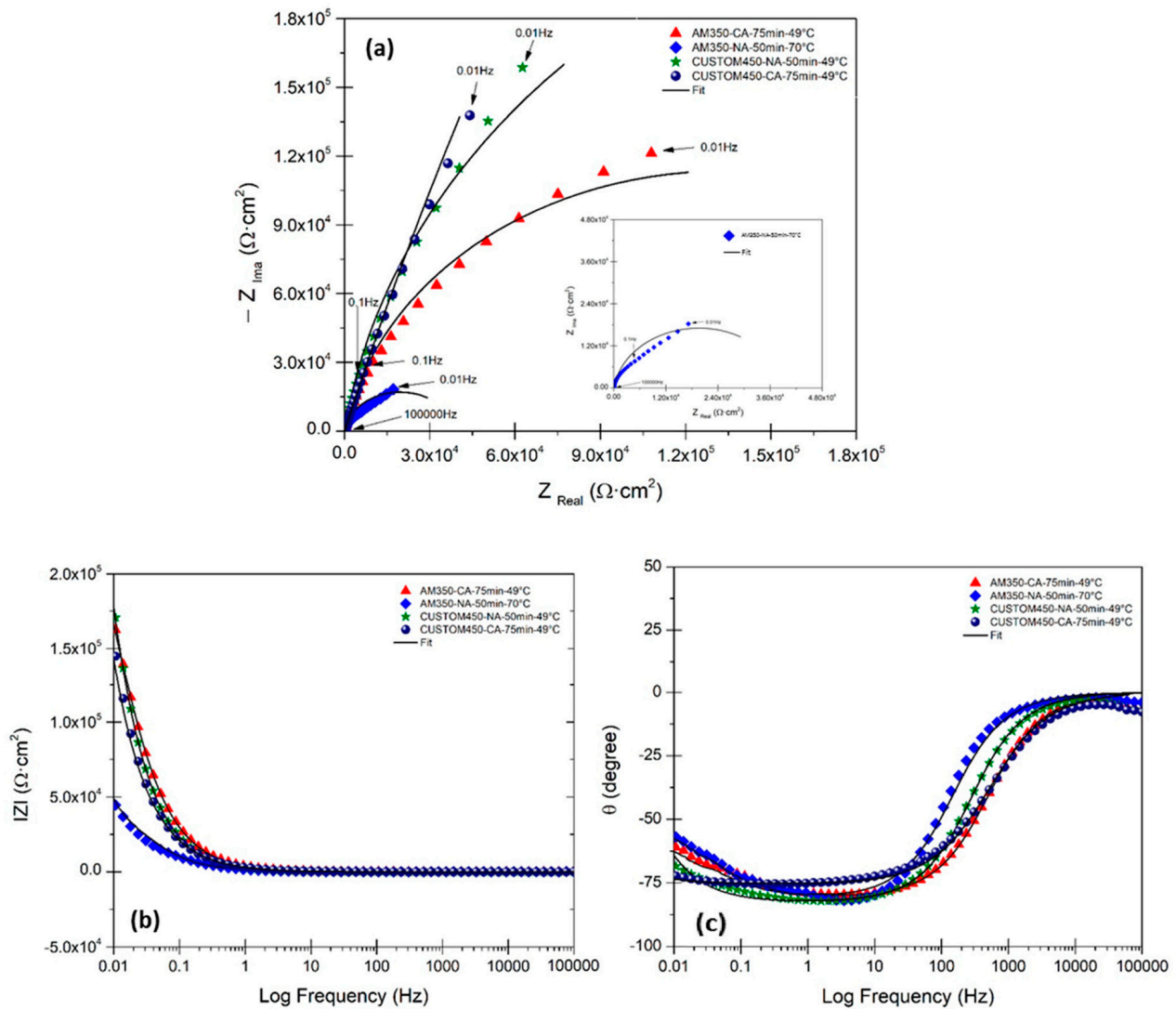
Figure 6. Nyquist (**a**) and Bode (**b**,**c**) plots of CUSTOM 450 and AM 350 passivated stainless steels immersed to 1 wt. % H_2SO_4 solution.

The physical and mathematical model of the metal/passive film/solution system is presented in Figure 7. The interface resistance is the resistance R1, and the passive electrode system is the capacitance C in parallel in the electrical equivalent circuit (EEC) [67–71]. The capacitance obtained can sometimes deviate from the "pure capacitance" when the actual system impedance is measured. A constant phase element (CPE) is introduced in data fitting to allow for depressed semicircles. The capacitor C is replaced with a CPE for better fit quality. Figure 7 proposes the following equivalent electrical circuit, where RS is the uncompensated solution resistance; R1 and CPE are the interface resistance and the constant phase element, respectively. The mathematical equation for the system impedance of HPSS steels in this model is [67].

$$Z = Rs + \frac{1}{\frac{1}{R} + Yo((j \cdot \omega)^n}$$

(8)

The constant phase element CPE impedance is presented by Equation (9) [72].

$$Z_{CPE} = \frac{1}{Yo(j \cdot \omega)^n}$$

(9)

where Y = admittance (the reciprocal of impedance), ω = angular frequency, $j^n = (-1)$ = imaginary number and n = dimensionless fraction exponent $(-1 < n < +1)$, constant phase element is an ideal capacitor (when $n = +1$) and is an inductor (when n = -1) [73–80].
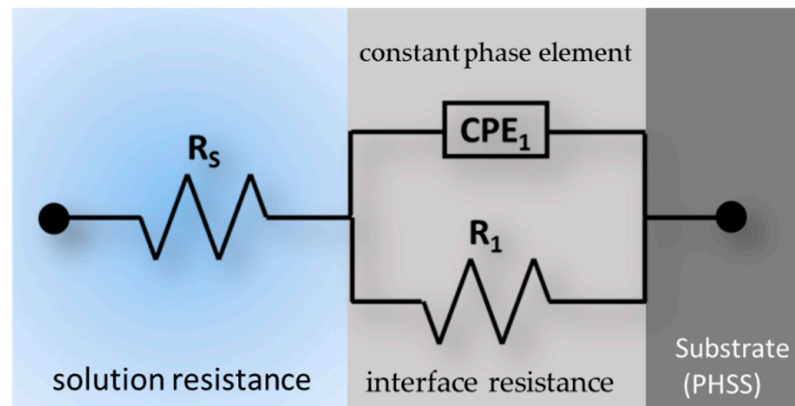

Figure 7. The proposed electrical equivalent circuit (EEC) model.

Tables 6 and 7 show the EIS parameters obtained by EEC simulation of AM350 and CUSTOM 450 passivated stainless sheets of steel immersed in 5 wt. % NaCl and 1 wt. % H_2SO_4 solution. The corresponding values of solution resistance Rs are in a range of 14.53–15.98 Ω·cm and show slight variation. For R1, the values presented are in a range of $3.915 \times 10^4 - 4252 \times 10^6$ Ω cm^2, where the CUSTOM450-NA-75min-70 °C passivated sample immersed in 1 wt. % H_2SO_4 solution had the highest charge transfer resistance. The lowest values of charge transfer resistance were recorded for samples AM350-NA-50min-70 °C (3.915×10^4 Ω·cm^2) and CUSTOM450-NA-75min-70 °C (3.555×10^5 Ω·cm^2) passivated in nitric acid. The passivated CUSTOM 450 stainless steel samples showed the best corrosion behavior in both test electrolytes.

Table 6. EIS parameters obtained by EEC simulation of CUSTOM 450 and AM 350 passivated stainless steels immersed to 5 wt. %NaCl solution.

Sample	R_s (Ω·cm)	R_1 (Ω·cm^2)	Y_1 (μs^{n1}·cm^{-2})	n_1	X^2
AM350-CA-50min-49 °C	14.57	1.0634×10^6	34.87	0.89	6.07×10^{-4}
AM350-NA-50min-70 °C	15.53	4.768×10^5	2.84	0.92	2.03×10^{-2}
CUSTOM450-NA-75min-70 °C	15.41	3.555×10^5	57.04	0.87	1.39×10^{-2}
CUSTOM 450-CA-50min-49 °C	15.98	1.326×10^6	1.31	0.95	1.73×10^{-2}

Table 7. EIS parameters obtained by EEC simulation of CUSTOM 450 and AM 350 passivated stainless steels immersed to 1 wt. % H_2SO_4 solution.

Sample	R_s (Ω·cm)	R_1 (Ω·cm^2)	Y_1 (μs^{n1}·cm^{-2})	n_1	X^2
AM350-CA-75min-49 °C	14.44	2.673×10^5	49.99	0.89	2.12×10^{-3}
AM350-NA-50min-70 °C	14.96	3.915×10^4	135.62	0.91	1.30×10^{-2}
CUSTOM 450-NA-50min-49 °C	16.04	5.88×10^5	64.87	0.91	2.47×10^{-3}
CUSTOM 450-CA-75min-49 °C	15.97	4.252×10^6	72.05	0.83	3.02×10^{-3}

4. Discussion

Electrochemical noise uses two data analysis methods: the time domain (statistical analysis) and the frequency domain (power spectral density, PSD). Those methods were employed to obtain information on the corrosion kinetics of passivated CUSTOM 450 and AM 350 precipitation hardened stainless steels immersed in NaCl and H_2SO_4 solutions.

In the time series of passivated stainless steels, the amplitude transients are associated with the corrosion kinetics, which decreased with time for steels immersed in the NaCl

solution. However, the PHSS immersed in H_2SO_4 solution showed transients associated with rupture and regeneration of the passive layer. This behavior is attributed to the anodic reactions of the OH^-. The R_n values are higher for AM 350 stainless steel in both passivation solutions, indicating a high corrosion resistance for this steel. On the other hand, the samples passivated in citric acid presented a lower corrosion resistance.

However, the samples passivated in nitric acid showed non-uniform passivation according to the LI values obtained, which corresponds to localized corrosion [5,29,47–49]. The type of corrosion that occurred for the passivated PHSS in both citric acid and nitric acid solutions indicates that the LI and asymmetry parameters were evaluated from the electrochemical noise data and found to be 0.003 to 0.2, see Table 1. The LI and skewness values obtained for the passivating solutions, the type of corrosion indicates localized corrosion due to the breakdown of the passive film. Various research groups have used the LI parameter [54–59], such as Cottis [53], as criteria to determine the possible type of corrosion occurring. In the present study, the LI and skewness parameters were estimated based on an analysis in the time domain and supported by an analysis in the frequency or time–frequency domain.

According to some authors [67,72,74], the impedance data obtained for passivated PHSS and exposed in sodium chloride and sulfuric acid solution were adequately represented by an equivalent electrical circuit model, comprising two elements: the interface resistance and the constant phase element in parallel and uncompensated solution resistance.

Macdonalds D. [81,82] indicates that EIS measurements allow obtaining information about the corrosion mechanism, establishing a theoretical transfer function, and developing the passive film growth model.

The passivation of stainless steel involves the formation of chromium and iron oxide films [83–87]. Dissolution on the steel surface generates a superficial enrichment of Cr^{3+}, giving rise to the formation of chromium trihydroxide $Cr(OH)_3$, as shown in Equation (10) and Figure 7. Further dissolution of the hydroxide leads to a continuous layer of Cr_2O_3, according to chemical reaction (5) [5,6,86–88]. Figure 8 shows a schematic diagram showing the corrosion mechanism for CUSTOM 450 and AM 350 stainless steels after passivation process in $C_6H_8O_7$ and HNO_3 baths.

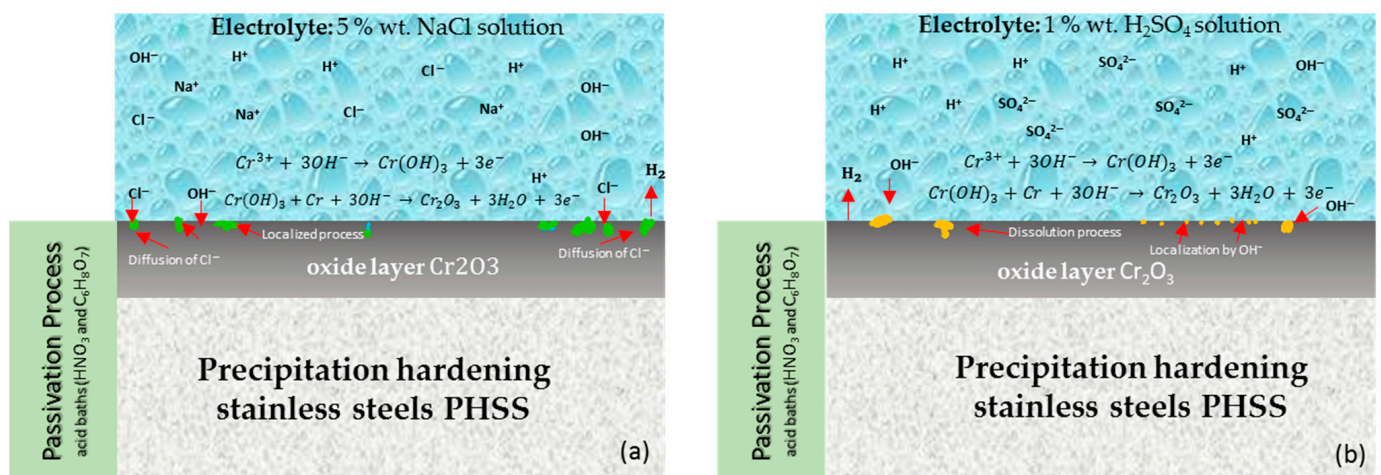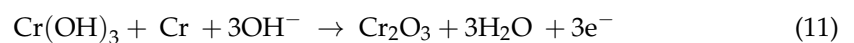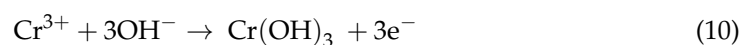$$Cr^{3+} + 3OH^- \rightarrow Cr(OH)_3 + 3e^- \tag{10}$$

$$Cr(OH)_3 + Cr + 3OH^- \rightarrow Cr_2O_3 + 3H_2O + 3e^- \tag{11}$$

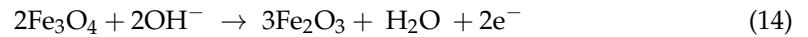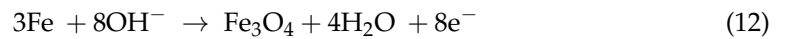**Figure 8.** Schematic diagram of passivation process in $C_6H_8O_7$ and HNO_3 bath for CUSTOM 450 and AM 350 stainless steels exposed to (**a**) 5 wt. % NaCl solution; (**b**) 1 wt. % H_2SO_4 solution.

According to the literature, the anodic reactions during the film growth period come mainly from the oxidation of iron and chromium. The following chemical reactions indicate the oxidation of iron [5,6,86,89,90]:

$$3Fe + 8OH^- \rightarrow Fe_3O_4 + 4H_2O + 8e^- \tag{12}$$

$$2Fe_3O_4 + 2OH^- + 2H_2O \rightarrow 6FeOOH + 2e^- \tag{13}$$

$$2Fe_3O_4 + 2OH^- \rightarrow 3Fe_2O_3 + H_2O + 2e^- \tag{14}$$

The samples passivated in nitric acid showed a higher trend of pitting corrosion. Noh et al. [91] conclude that nitric acid increases the chromium presence of the passive layer, removing MnS inclusions from the surface; also, the probability of individual pitting increases. In this research, the samples passivated in nitric acid presented more pitting than those passivated within citric acid due to the presence of MnS. To reduce the presence of MnS, changes in the acid concentration or the use of other solutions similar to citric acid, where the pitting process was more controlled, should be used.

$$MnS + 2H^+ \rightarrow Mn^{2+} + H_2S \tag{15}$$

$$2MnS + 3H_2O \rightarrow 2Mn^{2+} + S_2O_3^{2-} + 6H^+ + 8e^- \tag{16}$$
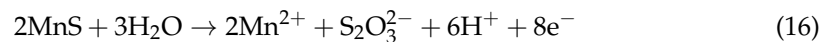
From the above reactions, MnS can be removed, and the passivation stability could be related to the acid concentration [92].

Research by Lara et al. and Gaydos et al. [5,22] conclude that citric acid can be used as an alternative to nitric acid since citric acid passivation showed better results compared to the nitric acid solution specified in AMS-QQ-P-35. Furthermore, citric acid helps to remove iron and some particle contamination; for this reason, samples passivated within citric acid presented a lower trend to localized process. Since the passivation process was not generated in preferential zones, the oxide layer formed will be more uniform, and because of this, it could be expected that the corrosion process will be one of uniform nature.

5. Conclusions

After studying the corrosion behavior of CUSTOM450 and AM350 stainless steels passivated in citric and nitric acid solutions for 50 and 75 min at 49 and 70 °C and exposed to 5 wt. % NaCl and 1 wt. % H_2SO_4 solutions, the following conclusions can be drawn:

- After evaluation by EN and irrespective of the method used, i.e., time domain (statistical analysis) and the frequency domain (power spectral density, PSD), PHSS samples passivated in citric acid showed lower corrosion resistance.
- AM 350 stainless steel passivated samples showed higher corrosion resistance than passivates of Custom 450 passivated stainless steel samples.
- Passivation in nitric acid baths made the surface prone to the localized corrosion process. In this condition, statistical and PSD values showed a tendency toward pitting corrosion.
- Passivated samples immersed in H_2SO_4 solution showed an increase in corrosion kinetics due to the breakdown and passivation of the passive layer.
- The samples passivated in citric acid showed lower corrosion resistance. However, samples passivated in nitric acid showed non-uniform passivation due to localized corrosion.
- The samples passivated in the citric acid bath and immersed in NaCl solution are the ones that presented the best corrosion behavior. Likewise, and from the EIS results the AM 350 passivated stainless steel samples immersed in H_2SO_4 solution presented the highest corrosion rates.
- The EIS results obtained for passivated PHSS have been fitted using an equivalent electrical circuit model where RS is the uncompensated solution resistance; R1 and CPE are the interface resistance and the constant phase element, respectively.

- On the whole, the results indicate the effectiveness of citric acid in the passivation of PH stainless steel, and its potential as an alternative to replacing nitric acid passivation solutions currently used in the aeronautical and aerospace industries.

References

1. Mouritz, P.A. *Introduction to Aerospace Materials*; Woodhead Publishing: Cambridge, UK, 2012.
2. Gloria, A.; Montanari, R.; Richetta, M.; Varone, A. Alloys for aeronautic applications: State of the art and perspectives. *Metals* **2019**, *9*, 662. [CrossRef]
3. Bocchetta, P.; Chen, L.-Y.; Tardelli, J.D.C.; Reis, A.C.D.; Almeraya-Calderón, F.; Leo, P. Passive layers and corrosion resistance of biomedical Ti-6Al-4V and β-Ti alloys. *Coatings* **2021**, *11*, 487. [CrossRef]
4. Cabral-Miramontes, J.A.; Barceinas-Sánchez, J.D.O.; Poblano-Salas, C.A.; Pedraza-Basulto, G.K.; Nieves-Mendoza, D.; Zambrano-Robledo, P.C.; Almeraya-Calderón, F.; Chacón-Nava, J.G. Corrosion behavior of AISI 409Nb stainless steel manufactured by powder metallurgy exposed in H_2SO_4 and NaCl solutions. *Int. J. Electrochem. Sci.* **2013**, *8*, 564–577.
5. Lara-Banda, M.; Gaona-Tiburcio, C.; Zambrano-Robledo, P.; Delgado, -E.M.; Cabral-Miramontes, J.A.; Nieves-Mendoza, D.; Maldonado-Bandala, E.; Estupiñán-López, F.; Chacón-Nava, J.G.; Almeraya-Calderón, F. Alternative to nitric acid passivation of 15-5 and 17-4PH stainless steel using electrochemical techniques. *Materials* **2020**, *13*, 2836. [CrossRef]
6. Lara Banda, M.; Gaona-Tiburcio, C.; Zambrano-Robledo, P.; Cabral, M.J.A.; Estupinan, F.; Baltazar-Zamora, M.A.; Almeraya-Calderon, F. Corrosion Behaviour of 304 Austenitic, 15–5PH and 17-4PH Passive Stainless Steels in acid solutions. *Int. J. Electrochem. Sci.* **2018**, *13*, 10314–10324. [CrossRef]
7. Gialanella, S.; Malandruccolo, A. *Aerospace Alloys*; Topics in Mining, Metallurgy and MaterialsEngineering; Bergmann, C.P., Ed.; Springer: Cham, Switzerland, 2020; ISSN 2364-3307. [CrossRef]
8. Lopes, J.C. Material selection for aeronautical structural application. *Sci. Technol. Adv. Mat.* **2008**, *20*, 78–82.
9. Lo, K.H.; Shek, C.H.; Lai, J.K.L. Recent developments in stainless steels. *Mat. Sci. Eng. R.* **2009**, *65*, 39–104. [CrossRef]
10. Cobb, H.M. *The History of Stainless Steel*; ASM International: Cleveland, OH, USA, 2010; pp. 189–192.
11. Ha, H.Y.; Jang, J.H.; Lee, T.H.; Won, C.; Lee, C.H.; Moon, J.; Lee, C.G. Investigation of the localized corrosion and passive behavior of type 304 stainless steels with 0.2–1.8 wt% B. *Materials* **2018**, *11*, 2097. [CrossRef]
12. Schmuki, P. From bacon to barriers: A review on the passivity of metal and alloys. *J. Solid. State Electr.* **2002**, *6*, 145–164. [CrossRef]
13. Abdelshehid, M.; Mahmodieh, K.; Mori, K.; Chen, L.; Stoyanov, P.; Davlantes, D.; Foyos, J.; Ogren, J.; Clark, R., Jr.; Es-Said, O.S. On the correlation between fracture toughness and precipitation hardening heat treatments in 15-5PH stainless steel. *Eng. Fail. Anal.* **2007**, *14*, 626–631. [CrossRef]
14. Esfandiari, M.; Dong, H. The corrosion and corrosion–wear behaviour of plasma nitrided 17-4PH precipitation hardening stainless steel. *Surf. Coat. Technol.* **2007**, *202*, 466–478. [CrossRef]
15. Dong, H.; Esfandiari, M.; Li, X.Y. On the microstructure and phase identification of plasma nitrided 17-4PH precipitation hardening stainless steel. *Surf. Coat. Technol.* **2008**, *202*, 2969–2975. [CrossRef]
16. Hsiao, C.N.; Chiou, C.S.; Yang, J.R. Aging reactions in a 17-4 PH stainless steel. *Mater. Chem. Phys.* **2002**, *74*, 134–142. [CrossRef]
17. Gladman, T. Precipitation hardening in metals. *Mater. Sci. Technol.* **1999**, *15*, 30–36. [CrossRef]
18. Schade, C.; Stears, P.; Lawley, A.; Doherty, R. Precipitation Hardening PM Stainless Steels. *Int. J. Powder Metall.* **2006**, *1*, 51–59.
19. Cobb, H.M. *The History of Stainless Steel*; ASM International: Geauga, OH, USA, 2010.
20. Farrar, J. *The Alloy Tree—A Guide to Low-Alloy Steels, Stainless Steels and Nickel-base Alloys*; Woodhead Publishing Limited and CRC Press: Sawston, UK, 2004.

21. *ASTM A967-17*; Standard Specification for Chemical Passivation Treatments for Stainless Steel Parts. ASTM International: West Conshohocken, PA, USA, 1999.
22. Gaydos, S.P. Passivation of aerospace stainless parts with citric acid solutions. *Plat. Surf. Finish.* **2003**, *90*, 20–25.
23. Shibata, T. Stochastic studies of passivity breakdown. *Corros. Sci. 1990. 31*, 413–423. [CrossRef]
24. Ashassi-Sorkhabi, H.; Seifzadeh, D.; Raghibi-Boroujeni, M. Analysis of electrochemical noise data in both time and frequency domains to evaluate the effect of ZnO nanopowder addition on the corrosion protection performance of epoxy coatings. *Arab. J. Chem.* **2016**, *9*, S1320–S1327. [CrossRef]
25. Isselin, J.; Kasada, R.; Kimura, A. Effects of aluminum on the corrosion behavior of 16% Cr ODS ferritic steels in a nitric acid solution. *J. Nucl. Sci. Techmol.* **2011**, *48*, 169–171. [CrossRef]
26. Corral, H.R.; Arredondo, R.S.P.; Neri, F.M.; Gómez, S.J.M.; Almeraya, C.F.; Castorena, G.J.H.; Almaral, S.J. Sulfate attack and reinforcement corrosion in concrete with recycled concrete aggregates and supplementary cementing materials. *Int. J. Electrochem. Sci.* **2011**, *6*, 613–621.
27. Bragaglia, M.; Cherubini, V.; Cacciotti, I.; Rinaldi, M.; Mori, S.; Soltani, P.; Nanni, F.; Kaciulis, S.; Montesperelli, G. Citric Acid Aerospace Stainless Steel Passivation: A Green Approach. In Proceedings of the CEAS Aerospace Europe Conference 2015, Delft, The Netherlands, 7–11 September 2015.
28. Suresh, G.U.; Kamachi, M.S. Electrochemical Noise Analysis of Pitting Corrosion of Type 304L Stainless Steel. *Corrosion.* **2014**, *70*, 283–293. [CrossRef]
29. Lara-Banda, M.; Ortiz, D.; Gaoan-Tiburcio, C.; Zambrano, P.; Cabral-Miramontes, J.C.; Almeraya-Calderon, F. Citric Acid Passivation of 15-5PH and 17-4PH Stainless Steel Used in the Aeronautical Industry. In *International Materials Research Congress*; Springer: Cham, Switzerland, 2016; pp. 95–104.
30. Tseng, K.H.; Chen, Y.C.; Chen, Y.C. Micro Plasma Arc Welding of AM 350 Precipitation Hardening Alloys. *Appl. Mech. Mater.* **2012**, *121*, 2681–2685. [CrossRef]
31. Shaikh, H.; George, G.; Khatak, H.S. Failure analysis of an AM 350 steel bellows. *Eng. Fail. Anal.* **2001**, *8*, 571–576. [CrossRef]
32. Warren, J.; Wei, D.Y. The low cycle fatigue behavior of the controlled transformation stainless steel alloy AM355 at 121, 204 and 315 °C. *Mater. Sci. Eng. A* **2008**, *475*, 148–156. [CrossRef]
33. Favor, R.J.; Deel, O.L.; Achbach, W.P. *Design Information on AM-350 Stainless Steel for Aircraft and Missiles*; Defense Metals Information Center, Battelle Memorial Institute: Columbus, OH, USA, 1961; Volume 156.
34. Kumar, T.S.; Ramanujam, R.; Vignesh, M.; Rohith, D.; Manoj, V.; Sankar, P.H. Comparative machining studies on custom 450 alloy with TiCN, TiAlN coated and uncoated carbide tools using Taguchi-Fuzzy logic approach. *Mater. Res. Express* **2019**, *6*, 066411. [CrossRef]
35. Lin, C.K.; Tsai, W.J. Corrosion fatigue behaviour of a 15Cr-6Ni precipitation-hardening stainless steel in different tempers. *Fatigue Fract. Eng. Mater. Struct.* **2000**, *23*, 489–497. [CrossRef]
36. Mollapour, Y.; Poursaeidi, E. Experimental and numerical analysis of Pitting Corrosion in CUSTOM 450 Stainless Steel. *Eng. Fail. Anal.* **2021**, *128*, 105589. [CrossRef]
37. Lin, C.K.; Chu, C.C. Mean stress effects on low-cycle fatigue for a precipitation-hardening martensitic stainless steel in different tempers. *Fatigue Fract. Eng. Mater. Struct.* **2000**, *23*, 545–553. [CrossRef]
38. AM 350 Technical Data. Available online: https://www.hightempmetals.com/techdata/hitempAM350data.php (accessed on 17 March 2022).
39. Custom 450® Stainless Steel. Available online: https://www.ulbrich.com/uploads/data-sheets/Custom-450-Stainless-Steel-Wire-UNS-S45000.pdf (accessed on 17 March 2022).
40. *ASTM E3-95*; Standard Practice for Preparation of Metallographic Specimens. ASTM International: West Conshohocken, PA, USA, 1995.
41. *ASTM A380-17*; Standard Practice for Cleaning, Descaling and Passivation of Stainless-Steel Parts, Equipment, and Systems. ASTM International: West Conshohocken, PA, USA, 1999.
42. Ramirez-Arteaga, A.M.; Gonzalez-Rodriguez, J.G.; Campillo, B.; Gaona-Tiburcio, C.; Dominguez-Patiño, G.; Leduc Lezama, L.; Chacon-Nava, J.G.; Neri-Flores, M.A.; Martinez-Villafañe, A. An electrochemical study of the corrosion behavior of a dual phase steel in 0.5m H_2SO_4. *Int. J. Electrochem. Sci.* **2010**, *5*, 1786–1798.
43. Olguin Coca, F.J.; Loya Tello, M.U.; Gaona-Tiburcio, C.; Romero, J.A.; Martínez-Villafañe, A.; Maldonado, B.E.; Almeraya-Calderón, F. Corrosion Fatigue of Road Bridges: A review. *Int. J. Electrochem. Sci.* **2011**, *6*, 3438–3451.
44. Samaniego-Gámez, P.; Almeraya-Calderón, F.; Martin, U.; Ress, J.; Gaona-Tiburcio, C.; Silva-Vidaurri, L.; Cabral-Miramontes, J.; Bastidas, J.M.; Chacón-Nava, J.G.; Bastidas, D.M. Efecto del tratamiento de sellado en el comportamiento frente a corrosión de la aleación anodizada de aluminio-litio AA2099. *Rev. Met.* **2020**, *56*, e180. [CrossRef]
45. *ASTM G106-15*; Standard Practice for Verification of Algorithm and Equipment for Electrochemical Impedance Measurements. ASTM International: West Conshohocken, PA, USA, 2010.
46. Macdonald, D.D. Review of mechanistic analysis by electrochemical impedance spectroscopy. *Electrochim. Acta* **1990**, *35*, 1509–1525. [CrossRef]
47. Gaona-Tiburcio, C.; Montoya-Rangel, M.; Cabral-Miramontes, J.A.; Estupiñán-López, F.; Zambrano-Robledo, P.; Orozco Cruz, R.; Chacón-Nava, J.G.; Baltazar-Zamora, M.A.; Almeraya-Calderón, F. Corrosion resistance of multilayer coatings deposited by PVD on Inconel 718 using electrochemical impedance spectroscopy technique. *Coatings* **2020**, *10*, 521. [CrossRef]

48. Arredondo-Rea, S.; Corral-Higuera, R.; Neri-Flores, M.A.; Gómez-Soberón, J.M.; Almeraya-Calderón, F.; Castorena-González, J.H.; Almaral-Sánchez, J. Electrochemical Corrosion and Electrical Resistivity of Reinforced Recycled Aggregate Concrete. *Int. J. Electrochem. Sci.* **2011**, *6*, 475–483.

49. Homborg, A.M.; Cottis, R.A.; Mol, J.M.C. An integrated approach in the time, frequency and time-frequency domain for the identification of corrosion using electrochemical noise. *Electrochim. Acta* **2016**, *222*, 627–640. [CrossRef]

50. Jaquez-Muñoz, J.; Gaona-Tiburcio, C.; Lira-Martinez, A.; Zambrano-Robledo, P.; Maldonado-Bandala, E.; Samaniego-Gamez, O.; Nieves-Mendoza, D.; Olguin-Coca, J.; Estupiñan-Lopez, F.; Almeraya-Calderon, F. Susceptibility to pitting corrosion of Ti-CP2, Ti-6Al-2Sn-4Zr-2Mo, and Ti-6Al-4V alloys for aeronautical applications. *Metals* **2021**, *11*, 1002. [CrossRef]

51. *ASTM G199-09*; Standard Guide for Electrochemical Noise Measurement. ASTM International: West Conshohocken, PA, USA, 2009.

52. Jáquez-Muñoz, J.M.; Gaona-Tiburcio, C.; Cabral-Miramontes, J.; Nieves-Mendoza, D.; Maldonado-Bandala, E.; Olguín-Coca, J.; López-Léon, L.D.; Flores-De los Rios, J.P.; Almeraya-Calderón, F. Electrochemical noise analysis of the corrosion of titanium alloys in NaCl and H_2SO_4 solutions. *Metals* **2021**, *11*, 105. [CrossRef]

53. Cottis, R.; Turgoose, S.; Mendoza-Flores, J. The effects of solution resistance on electrochemical noise resistance measurements: A theorical analysis. In *Electrochemical Noise Measurement for Corrosion Applications STP 1277*; Kearns, J.R., Scully, J.R., Roberge, P.R., Reirchert, D.L., Dawson, L., Eds.; ASTM International, Materials Park: West Conshohocken, PA, USA, 1996; pp. 93–100.

54. Eden, D.A. Electrochemical noise—The first two octaves. In *Corrosion/98*; NACE: San Diego, CA, USA, 1998; pp. 1–31.

55. Gaona-Tiburcio, C.; Aguilar, L.M.R.; Zambrano-Robledo, P.; Estupiñán-López, F.; Cabral-Miramontes, J.A.; Nieves-Mendoza, D.; Castillo-González, E.; Almeraya-Calderón, F. Electrochemical noise analysis of nickel based superalloys in acid solutions. *Int. J. Electrochem. Sci.* **2014**, *9*, 523–533.

56. Montoya-Rangel, M.; De Garza-Montes, O.N.; Gaona-Tiburcio, C.; Colás, R.; Cabral-Miramontes, J.; Nieves-Mendoza, D.; Maldonado-Bandala, E.; Chacón-Nava, J.; Almeraya-Calderón, F. Electrochemical noise measurements of advanced high-strength steels in different solutions. *Metals* **2020**, *10*, 1232. [CrossRef]

57. Dawson, D.L. Electrochemical noise measurement: The definitive in-situ technique for corrosion applications. In *Electrochemical Noise Measurement for Corrosion Applications STP 1277*; Kearns, J.R., Scully, J.R., Roberge, P.R., Reirchert, D.L., Dawson, L., Eds.; ASTM International, Materials Park: West Conshohocken, PA, USA, 1996; pp. 3–39.

58. Wagner, C.; Traud, W. *Über Die Deutung Von Korrosionsvorgängen Durch Überlagerung Von elektrochemischen Teilvorgängen Und Über die Potentialbildung an Mischelektroden, Z. Elektrochem*; Springer: Berlin/Heidelberg, Germany, 1951; pp. 391–454. [CrossRef]

59. Butler, J.A.V. Studies in heterogeneous equilibria. Part II.—The kinetic interpretation on the Nernst theory of electromotive force. *Trans. Faraday Soc.* **1924**, *19*, 729–733. [CrossRef]

60. Monticelli, C. Evaluation of corrosion inhibitors by electrochemical noise analysis. *J. Electrochem. Soc.* **1992**, *139*, 706. [CrossRef]

61. Park, C.J.; Kwon, H.S. Electrochemical noise analysis of localized corrosion of duplex stainless steel aged at 475 °C. *Mater. Chem. Phys.* **2005**, *91*, 355–360. [CrossRef]

62. Gaona-Tiburcio, C.; Almeraya-Calderón, F.; Chacon-Nava, J.; Matutes-Aquino, A.M.; Martinez-Villafañe, A. Electrochemical response of permanent magnets in different solutions. *J. Alloys Compd.* **2004**, *369*, 78–80. [CrossRef]

63. Cabral-Miramontes, J.A.; Gaona-Tiburcio, C.; Almeraya-Calderón, F.; Estupiñan-Lopez, H.F.; Pedraza-Basulto, G.; Poblano-Salas, C. Parameter studies on high-velocity oxy-fuel spraying of CoNiCrAlY coatings used in the aeronautical industry. *Int. J. Corros.* **2014**, *2014*, 703806. [CrossRef]

64. Coakley, J.; Vorontsov, V.A.; Littlell, K.C.; Heenan, R.K.; Ohnuma, G.; Jones, N.G.; Dye, D. Nanoprecipitation in a beta-titanium alloy. *J. Alloys Compd.* **2015**, *623*, 146. [CrossRef]

65. Bertocci, U.; Huet, F. Noise analysis applied to electrochemical systems. *Corrosion* **1995**, *51*, 131–144. [CrossRef]

66. Mehdipour, M.; Naderi, R.; Markhali, B.P. Electrochemical study of effect of the concentration of azole derivatives on corrosion behavior of stainless steel in H_2SO_4. *Prog. Org. Coat.* **2014**, *77*, 1761–1767. [CrossRef]

67. Fattah-alhosseini, A.; Taheri Shoja, S.; Heydari Zebardast, B.; Mohamadian Samim, P. An Electrochemical Impedance Spectroscopic Study of the Passive State on AISI 304 Stainless Steel. *Int. J. Electrochem* **2011**, *2011*, 8. [CrossRef]

68. Castro, B.E.; Vilche, R.J. Investigation of passive layers on iron and iron-chromium alloys by electrochemical impedance spectroscopy. *Electrochim. Acta* **1993**, *38*, 1567–1572. [CrossRef]

69. Ge, H.H.; Zhou, G.D.; Wu, W.Q. Passivation model of 316 stainless steel in simulated cooling water and the effect of sulfide on the passive film. *Appl. Surf. Sci.* **2003**, *211*, 321–334. [CrossRef]

70. Ameer, A.M.; Fekry, M.A.; Heakal, T.E.F. Electrochemical behaviour of passive films on molybdenum-containing austenitic stainless steels in aqueous solutions. *Electrochim. Acta* **2004**, *50*, 43–49. [CrossRef]

71. Ningshen, S.; Mudali, K.U.; Amarendra, G.; Gopalan, P.; Dayal, K.R.; Khatak, S.H. Hydrogen effects on the passive film formation and pitting susceptibility of nitrogen containing type 316L stainless steels. *Corros. Sci.* **2006**, *48*, 1106–1121. [CrossRef]

72. Bastidas, D.M. Interpretation of impedance data for porous electrodes and diffusion processes. *Corrosion* **2007**, *63*, 515–521. [CrossRef]

73. Samaniego-Gámez, P.O.; Almeraya-Calderon, F.; Maldonado-Bandala, E.; Cabral-Miramontes, J.; Nieves-Mendoza, D.; Olguin-Coca, J.; Lopez-Leon, L.D.; Silva Vidaurri, L.G.; Zambrano-Robledo, P.; Gaona-Tiburcio, C. Corrosion Behavior of AA2055 Aluminum-Lithium Alloys Anodized in the Presence of Sulfuric Acid Solution. *Coatings* **2021**, *11*, 1278. [CrossRef]

74. Scully, J.R.; Silverman, D.C.; Kendig, M.W. *Electrochemical Impedance: Analysis and Interpretation STP 1188*; ASTM International: Philadelphia, PA, USA, 1993. [CrossRef]

75. Pérez, N. *Electrochemistry and Corrosion Science*; Springer: New York, NY, USA, 2004.

76. Hirschorn, B.; Orazem, M.E.; Tribollet, B.; Vivier, V.; Frateur, I.; Musiani, M. Determination of effective capacitance and film thickness from constant-phase-element parameters. *Electrochim. Acta* **2010**, *55*, 6218–6227. [CrossRef]

77. Evertsson, J.; Bertram, F.; Rullik, L.; Harlow, G.; Lundgren, E. Anodization of Al (100), Al (111) and Al Alloy 6063 studied in situ with X-ray reflectivity and electrochemical impedance spectroscopy. *J. Electroanal. Chem.* **2017**, *799*, 556–562. [CrossRef]

78. Corral-Higuera, R.; Arredondo-Rea, P.; Neri-Flores, M.A.; Gómez-Soberón, J.M.; Almaral-Sánchez, J.L.; Castorena-González, J.C.; Almeraya-Calderón, F. Chloride ion penetrability and corrosion behavior of steel in concrete with sustainability characteristics. *Int. J. Electrochem. Sci.* **2011**, *6*, 958–970.

79. Ayagou, M.D.D.; Tran, T.T.M.; Tribollet, B.; Kittel, J.; Sutter, E.; Ferrando, N.; Mendibide, C.; Duret-Thual, C. Electrochemical impedance spectroscopy of iron corrosion in H_2S solutions. *Electrochim. Acta* **2018**, *282*, 775–783. [CrossRef]

80. Núñez-Jaquez, R.E.; Buelna-Rodríguez, J.E.; Barrios-Durstewitz, C.P.; Gaona-Tiburcio, C.; Almeraya-Calderón, F. Corrosion of modified concrete with sugar cane bagasse ash. *Int. J. Corros.* **2012**, *2012*, 451864. [CrossRef]

81. Macdonald, D.D. Point defect model for the passive state. *J. Electrochem. Soc.* **1992**, *139*, 3434–3449. [CrossRef]

82. Macdonald, D.D.; Smedley, S.I. An electrochemical impedance analysis of passive films on nickel(111) in phosphate buffer solutions. *Electrochim. Acta* **1990**, *35*, 1949–1956. [CrossRef]

83. Fattah-alhosseini, A.; Saatchi, A.; Golozar, M.A.; Raeissi, K. The transpassive dissolution mechanism of 316L stainless steel. *Electrochim. Acta* **2009**, *54*, 3645–3650. [CrossRef]

84. Man, C.; Dong, C.; Cui, Z.; Xiao, K.; Yu, Q.; Li, X. A comparative study of primary and secondary passive films formed on AM355 stainless steel in 0.1 M NaOH. *Appl. Surf. Sci.* **2018**, *427*, 763–773. [CrossRef]

85. Bojinov, M.; Betova, I.; Fabricius, G.; Laitinen, T.; Saario, T. The stability of the passive state of iron–chromium alloys in sulphuric acid solution. *Corros. Sci.* **1999**, *41*, 1557–1584. [CrossRef]

86. Bojinov, M.; Fabricius, G.; Kinnunen, P.; Laitinen, T.; Mäkelä, K.; Saario, T.; Sundholm, G. The mechanism of transpassive dissolution of Ni–Cr alloys in sulphate solutions. *Electrochim. Acta.* **2000**, *45*, 2791–2802. [CrossRef]

87. Huang, J.; Wu, X.; Han, E.H. Electrochemical properties and growth mechanism of passive films on Alloy 690 in high-temperature alkaline environments. *Corros. Sci.* **2010**, *52*, 3444–3452. [CrossRef]

88. Calinski, C.; Strehblow, H.H. ISS depth profiles of the passive layer on Fe/Cr alloys. *J. Electrochem. Soc.* **1989**, *36*, 1328–1331. [CrossRef]

89. Martinez-Villafane, A.; Chacon-Nava, J.G.; Gaona-Tiburcio, C.; Almeraya-Calderon, F.; Dominguez-Patino, G.; Gonzalez-Rodriguez, J.G. Oxidation performance of a Fe–13Cr alloy with additions of rare earth elements. *Mater. Sci. Eng. A* **2003**, *363*, 15–19. [CrossRef]

90. Cabral Miramontes, J.A.; Barceinas Sánchez, J.D.O.; Almeraya Calderón, F.; Martínez Villafañe, A.; Chacón Nava, J.G. Effect of Boron Additions on Sintering and Densification of a Ferritic Stainless Steel. *J. Mater. Eng. Perform.* **2010**, *19*, 880–884. [CrossRef]

91. Noh, L.S.; Laycock, N.J.; Gao, W.; Wells, D.B. Effects of nitric acid passivation on the pitting resistance of 316 stainless steel. *Corros. Sci.* **2000**, *42*, 2069–2084. [CrossRef]

92. Brossia, C.S.; Kelly, R.G. On the role of alloy sulfur in the initiation of crevice corrosion in stainless steel. In *Critical Factors in Localized II*; Natishan, P.M., Kelly, R.G., Frankel, G.S., Newman, R.C., Eds.; The Electrochemical Society: Pennington, NJ, USA, 1996; Volume 95–115, pp. 201–217.